COMPARISON OF 2D AND 3D SIMULATIONS OF AN OWC DEVICE IN DIFFERENT CONFIGURATIONS

Arun Kamath [1], Hans Bihs [2], Øivind A. Arntsen [3]

The oscillating water column (OWC)device is a wave energy converter which converts the work done by the air column in a partially submerged pneumatic chamber into a electrical energy. This paper carries out numerical simulations using a computation fluid dynamics model to study the motion of the free surface inside the chamber in two different configurations of the device and also in two- and three-dimensions. It is observed that the 2D and 3D simulations provide the same results for the motion of the free surface and thus computationally cheaper 2D simulations can be employed to study the hydrodynamics of the OWC device. It is also observed that an asymmetrical device produces higher oscillation of the free surface in the chamber as it does not allow transmission of the wave across the device as in a symmetrical configuration.

Keywords: OWC; CFD; 3D simulations

INTRODUCTION

A good understanding of the hydrodynamics of Oscillating Water Column (OWC) devices is essential before their commercial deployment to harvest ocean wave energy. Evans (1978) analytically calculated the efficiency of a wave energy converter device modelled as a pair of parallel vertical plates with a float connected to a spring-dashpot on the free surface as the wave energy absorber. Further, an adaptation of the theory for rigid oscillating bodies was used to determine the power absorption in an OWC device by Evans (1982). Sarmento and Falcão (1985) analysed an OWC device in two dimensions considering linearised spring-like air compressibility and pointed at air compressibility being an important factor in practice.
Sarmento (1992) also carried out wave flume experiments on an OWC device and studied both linear and quadratic power take off mechanisms using filters and an orifice plate respectively. Morris-Thomas et al. (2007) carried out experiments to determine the hydrodynamic efficiency of an OWC device with varying wall thickness, draught of the front wall for various wave parameters. Thiruvenkatasamy and Neelamani (1997) studied the effect of nozzle area on the efficiency of an OWC device through wave flume experiments. They reported that for nozzle areas greater than 0.81% of the free surface area, there was a dramatic drop in the efficiency of the OWC device due to very low pressures developed in the chamber.
In terms of numerical simulations with OWC devices, there have been a few studies which have used potential theory and the Boundary Element Method (BEM) to analyze the hydrodynamics of the device. Hong et al. (2007) experimentally examined the effects of air duct width, chamber length, skirt thickness and variation of bottom slope. They postulated that the dominance of pneumatic damping reduces for larger chamber volumes. Koo and Kim (2010) carried out numerical experiments using the BEM method and used viscous damping terms in the model.
In recent times, Computational Fluid Dynamics (CFD) has also been utilised to understand the hydrodynamics of the OWC device studying the two phase flow of air and water. Liu et al. (2008) studied the effect of the chamber-duct on the relative amplitude of the inner water surface and the air flow through the nozzle. Senturk and Ozdamar (2011) analyzed a simplified theoretical model of the Japanese OWC device Kaimei and reported a deviation of up to 30% between the analytical solution and the numerical result for nozzle velocity. Zhang et al. (2012) numerically replicated the experiments of Morris-Thomas et al. (2007) and reported over prediction of the efficiency due to complex pressure changes in the chamber around resonance. It has to be noted that the use of a nozzle in an experiment is to simulate non-linear external damping and the nozzle width determines the amount of damping on the chamber. Didier et al. (2011) demonstrated numerical experiments without providing a nozzle and directly using a linear pressure drop law to account for the external damping using CFD.
The objective of this paper is to explore the difference in the device hydrodynamics for symmetrical and asymmetrical configurations of the device. The symmetrical configuration of the device has walls of equal submergence both in front and behind the device and allows for wave transmission across the device. In an asymmetrical configuration, the back wall extends to the sea bed and obstructs wave transmission. The difference between a three-dimensional and two-dimensional simulation is also explored to determine whether

[1]Department of Civil and Transport Engineering, Norwegian University of Science and Technology, Norway
[2]Department of Civil and Transport Engineering, Norwegian University of Science and Technology, Norway
[3]Department of Civil and Transport Engineering, Norwegian University of Science and Technology, Norway

a computationally cheaper two-dimensional simulation is sufficient to analyse the chamber hydrodynamics of the OWC device.

NUMERICAL MODEL

Governing Equations

The open source CFD code employed in this study, REEF3D, solves the fluid flow problem using the incompressible Reynolds-Averaged Navier-Stokes (RANS) equations:

$$\frac{\partial U_i}{\partial x_i} = 0 \tag{1}$$

$$\frac{\partial U_i}{\partial t} + U_j \frac{\partial U_i}{\partial x_j} = -\frac{1}{\rho}\frac{\partial P}{\partial x_i} + \frac{\partial}{\partial x_j}\left[(\nu + \nu_t)\left(\frac{\partial U_i}{\partial x_j} + \frac{\partial U_j}{\partial x_i}\right)\right] + g_i \tag{2}$$

where U is the velocity averaged over time t,ρ is the fluid density, P is the pressure ν is the kinematic viscosity, ν_t is the eddy viscosity and g the acceleration due to gravity.
The Poisson pressure equation is discretized using the projection method proposed by Chorin (1968) and then a preconditioned BiCGStab iterative solver developed by van der Vorst (1992) is used to obtain the values for pressure. Turbulence modelling is handled using the two equation k-ω model proposed by Wilcox (1994) with modifications suggested by Durbin (2009), with the transport equations for k and ω defined by:

$$\frac{\partial k}{\partial t} + U_j \frac{\partial k}{\partial x_j} = \frac{\partial}{\partial x_j}\left[\left(\nu + \frac{\nu_t}{\sigma_k}\right)\frac{\partial k}{\partial x_j}\right] + P_k - \beta_k k\omega \tag{3}$$

$$\frac{\partial \omega}{\partial t} + U_j \frac{\partial \omega}{\partial x_j} = \frac{\partial}{\partial x_j}\left[\left(\nu + \frac{\nu_t}{\sigma_\omega}\right)\frac{\partial \omega}{\partial x_j}\right] + \frac{\omega}{k}\alpha P_k - \beta\omega^2 \tag{4}$$

where P_k is the production rate, closure coefficients α=$\frac{5}{9}$ β_k = $\frac{9}{100}$and β=$\frac{3}{40}$.

Eddy viscosity, ν_t, is bounded to avoid unphysical overproduction of turbulence in strained flow as shown by Durbin (2009):

$$\nu_t \leq \sqrt{\frac{2}{3}}\frac{k}{|\mathbf{S}|} \tag{5}$$

where $\mathbf{S}$ stands for the source terms in the transport equations for k and ω. The large difference at the interface between air and water leads to overproduction of turbulence at the interface due to increased strain. To avoid unphysical production of turbulence, free surface damping is introduced with a limiter around the interface for the source terms as shown by Menter (1992) and incorporated by Höhne and Vallée (2008). The limiter is activated around the interface for a thickness of 2ϵ by multiplying the Dirac delta function to the source term.

The fifth order conservative finite difference Weighted Essentially Non-Oscillatory (WENO) scheme proposed by Jiang and Shu (1996) is used for discretization of convective terms for the velocity U_i, the level set function ϕ, turbulent kinetic energy k and the specific turbulent dissipation rate ω. This higher-order scheme provides the accuracy required to model complex free surface flows and has numerical stability from its non-oscillatory property. A TVD third order Runge-Kutta explicit time scheme developed by Harten (1983) is employed for time advancement of the level set function and the reinitialisation equation. The model uses a Cartesian grid for spatial discretization. This facilitates a straight forward implementation of the finite difference schemes. The boundary conditions for complex geometries are handled using an adaptation of the Immersed Boundary Method (IBM), a method initially proposed for elastic boundaries by Peskin (1972). This was further developed by Tseng and Ferziger (2003) to a ghost cell IBM, where the values from the fluid region are extrapolated along the orthogonal to the boundary into the solid region using cells called ghost cells. As an improvement, a local directional ghost cell approach was adopted by Berthelsen and Faltinsen (2008). In the current study, a multiple ghost cell IBM (MGCIBM) implemented by Bihs (2011) using object oriented programming techniques is used, where the ghost cell values can be updated from multiple directions. The ghost cells store multiple values and return a particular value when called from a particular direction. The domain is decomposed into smaller pieces and a processor is assigned to each part. So, the program runs separately on each processor and the values between the processes are communicated using the MPI library.

Level Set Method

The free surface is obtained using the level set method. In this method, the zero level set of a signed distance function, $\phi(\vec{x},t)$ called the level set function, represents the interface between water and air. For the rest of the domain, the level set function represents the closest distance of the point from the interface and the sign distinguishes the two fluids across the interface. The level set function is defined as:

$$\phi(\vec{x},t)\begin{cases} > 0 & if\ \vec{x}\ is\ in\ phase\ 1 \\ = 0 & if\ \vec{x}\ is\ at\ the\ interface \\ < 0 & if\ \vec{x}\ is\ in\ phase\ 2 \end{cases} \tag{6}$$

The motion of the interface is represented by convecting the level set function using:

$$\frac{\partial \phi}{\partial t} + \vec{u}\nabla\phi = 0 \tag{7}$$

The signed distance property of the level set function is lost when the interface moves. A PDE based reinitialisation procedure presented by Sussman et al. (1994) is then used to restore the signed distance property of the function. The property of the level set function being smooth across the interface provides a sharp description of the free surface.

Numerical Wave Tank

The wave generation and wave absorption in the numerical wave tank is carried out by a relaxation method. The concept was proposed by Larsen and Dancy (1983), where the analytical solution is used to moderate the computationally generated waves in the wave tank. This procedure of moderating the values is called relaxation and has been presented by Mayer et al. (1998) and Engsig-Karup (2006). Here, the values of velocity and the free surface are moderated in the relaxation zones for wave generation and absorption zones using the following equations:

$$\begin{aligned} U_{relaxed} &= \Gamma(x)U_{analytical} + (1-\Gamma(x))U_{computational} \\ \phi_{relaxed} &= \Gamma(x)\phi_{analytical} + (1-\Gamma(x))\phi_{computational} \end{aligned} \tag{8}$$

where $\Gamma(x)$ is called the relaxation function and $x \in [0,1]$ is the measure along the relaxation zone.
The relaxation function is a smooth function with a range $[0,1]$ such that it facilitates smooth transition between the computational and analytical values in the relaxation zones. In this study, the set of relaxation functions presented by Engsig-Karup (2006) for wave generation and absorption is used:

$$\begin{aligned} \Gamma(x) = -2x^3 + 3x^2 \text{ for } x \in [0,1] \\ \Gamma(x) = 1 - x^6 \end{aligned} \tag{9}$$

In the wave generation zone, the computational values of velocity and free surface are taken from zero to the analytical values expected using the appropriate wave theory using Eqn. (8). The first relaxation function transitions the values of velocity and free surface to values prescribed by the wave theory, waves are generated and released into the wave tank. At the numerical beach, the values for the same variables are to be zero as all the energy is expected to be damped from the computational values existing in the wave tank. The second relaxation function is used at the beach and it ensures that the energy in the wave tank is smoothly removed by reducing the computational values smoothly without generating waves propagating in the opposite direction.

RESULTS AND DISCUSSION

At first, a grid refinement study is carried out. Linear waves of wavelength $\lambda = 2$m and wave height of 0.02 m are generated in the wave tank with a water depth of $d = 0.5$m at grid sizes $dx = 0.1$m, 0.05 m, 0.025 m and 0.01m. The results are presented in 1 and is observed that as the grid is refined, the wave height conforms to the prescribed value from linear wave theory with similar waveforms for grid sizes of $dx = 0.025$m and $dx = 0.01$m. So, a grid size of $dx = 0.025$m is considered to be sufficient to simulate wave interaction with OWC devices.

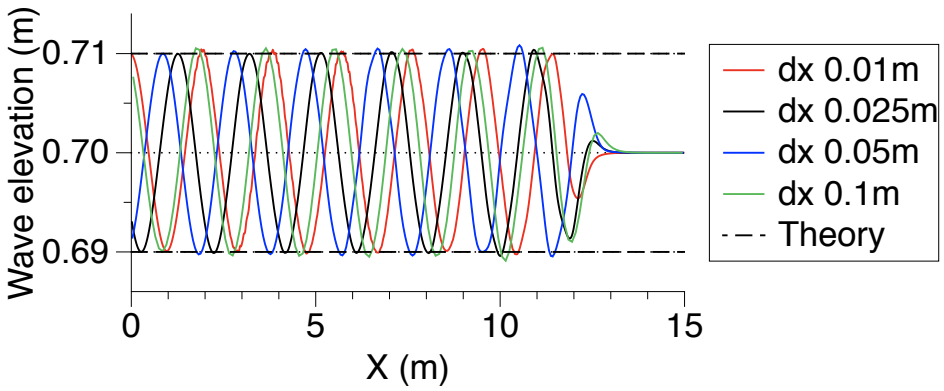

Figure 1: Grid refinement study

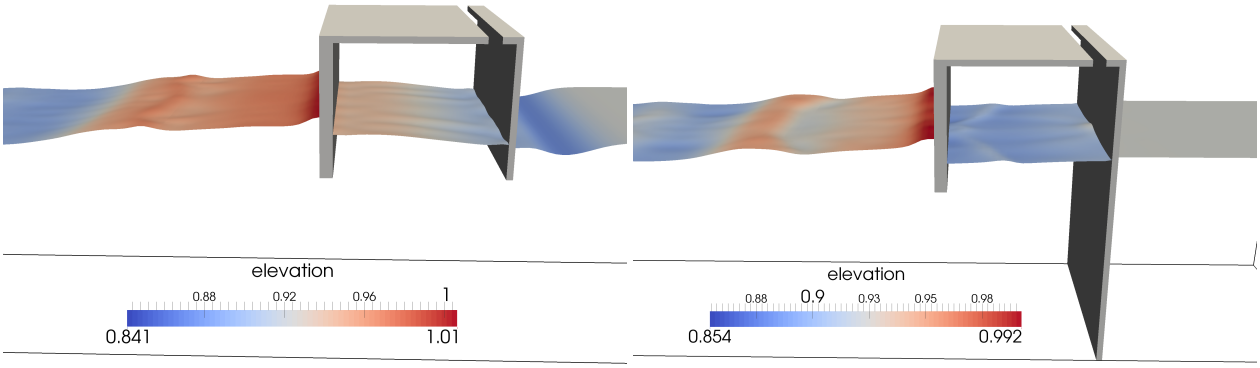

(a) Symmetrical setup **(b)** Asymmetrical setup

Figure 2: Two different configurations of the OWC device

Simulations are then carried out in two and three dimensions for two different configurations of the OWC device. In the symmetrical configuration as shown in Fig.2a, the depth of submergence of both the front and the back walls is the same. In the asymmetrical configuration as shown in Fig.2b, the back wall extends to the bottom whereas the front wall has a certain depth of submergence. The dimensions of the device are taken from the experiments carried out by Morris-Thomas et al. (2007). In the three-dimensional case, the width of the device is taken to be equal to the width of the numerical wave flume that is, $1m$. In this way, any three dimensional effects due inside the chamber due to motion of fluid in the chamber is studied, without influence from the fluid motion outside the device.

Symmetrical configuration

Linear waves with wave height 0.12 m and wavelengths (λ): 1.92m, 2.28m, 2.80m, 3.56m, 4.23m and 4.82m are simulated in the wave tank. The results for incident wavelengths λ = 1.92m, λ = 3.56m, λ = 4.23m and λ = 4.82m are shown in Figs.3a, 3b, 3c and 3d respectively. It is seen that the amplitude of oscillation inside the chamber increases with increasing incident wavelength.

Next, a three-dimensional simulation is carried out for the case with incident wavelength $\lambda = 3.56m$ and the free surface motion at the centre of the chamber in both the simulations is studied. It is observed that the free surface motion in both the 2D and the 3D simulation are the same in Fig.4. Thus, a 2D simulation provides the same information regarding the fluid motion inside the device chamber as a 3D simulation for a symmetrical OWC device.

Asymmetrical configuration

Further, simulations are carried out with the same wave parameters for the asymmetrical configuration. The free surface motion calculated by the numerical model for incident wavelengths of λ = 1.92m, λ =

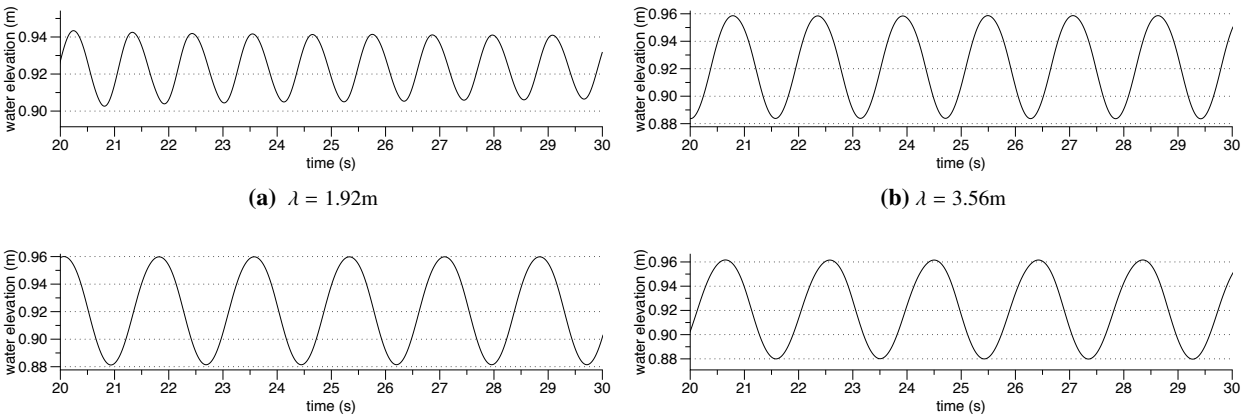

(a) λ = 1.92m **(b)** λ = 3.56m

(c) λ = 4.26m **(d)** λ = 4.82m

Figure 3: Free surface oscillations in the chamber in a two-dimensional simulation for different incident wavelengths for the symmetrical configuration

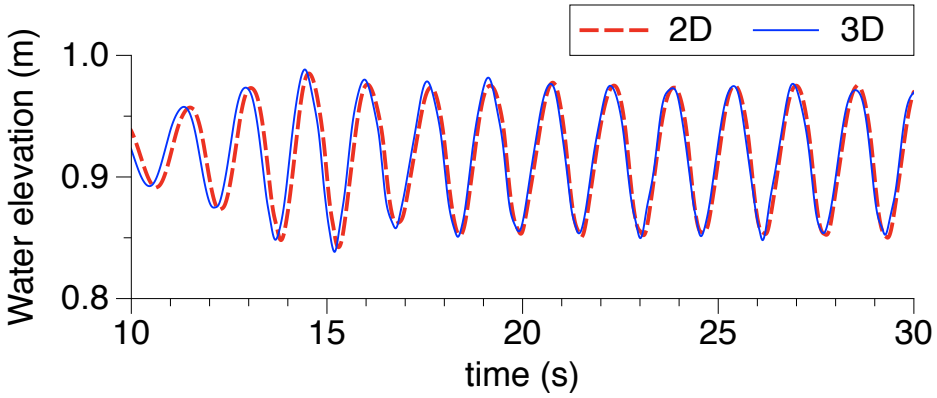

Figure 4: Comparison of free surface motion in 2D and 3D simulations at λ = 3.56m for the symmetrical configuration

3.56m, λ = 4.26m and λ = 4.82m are presented in Figs.5a, 5b, **??** and 5d respectively. The increase in free surface motion with increasing wavelength seen in the case of the symmetrical configuration is seen in the case of the asymmetrical configuration as well. It is also observed that the amplitudes of oscillation in these cases is higher than seen for the symmetrical case or every incident wavelength. This is as expected from the fact that in an asymmetrical configuration, the incident wave cannot be transmitted across the device as in the case of the symmetrical configuration.

The interaction of the asymmetrical configuration with an incident wavelength of λ = 3.56m is then studied in a three-dimensional numerical wave tank. It is observed that the free surface motion in this configuration is also the same for both 2D and 3D simulations. Thus, computationally cheaper 2D simulations can be used to analyze the fluid flow inside the chamber of an OWC device.

In order to further understand the influence of the back wall on the fluid flow inside the chamber, the water particle motion inside the device chamber is studied. It is seen in Fig.7a that the water particles enter and exit the chamber in the symmetrical configuration with only small zones of stagnation around the two walls of the chamber. On the other hand, in the case of an asymmetrical configuration, a large zone of stagnation is seen in the center of the chamber due to the influence of the back wall. The incident waves diffract around the front wall, get reflected by the back wall and these fluid motions mix with the upward motion of the free surface inside the chamber resulting in a complex flow inside the chamber with large zones of stagnation as seen in Fig.7b.

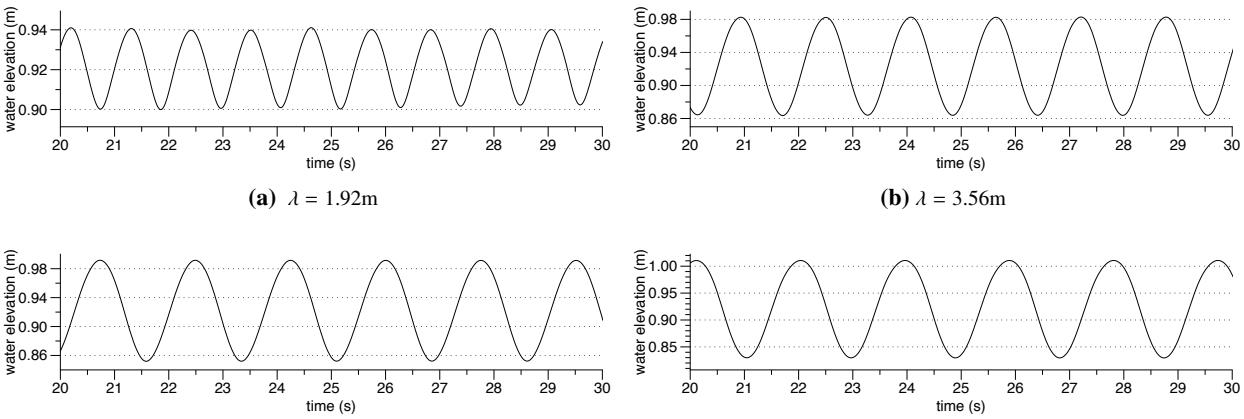

(a) $\lambda = 1.92$m **(b)** $\lambda = 3.56$m

(c) $\lambda = 4.26$m **(d)** $\lambda = 4.82$m

Figure 5: Free surface oscillations in the chamber in a two-dimensional simulation for different incident wavelengths for the asymmetrical configuration

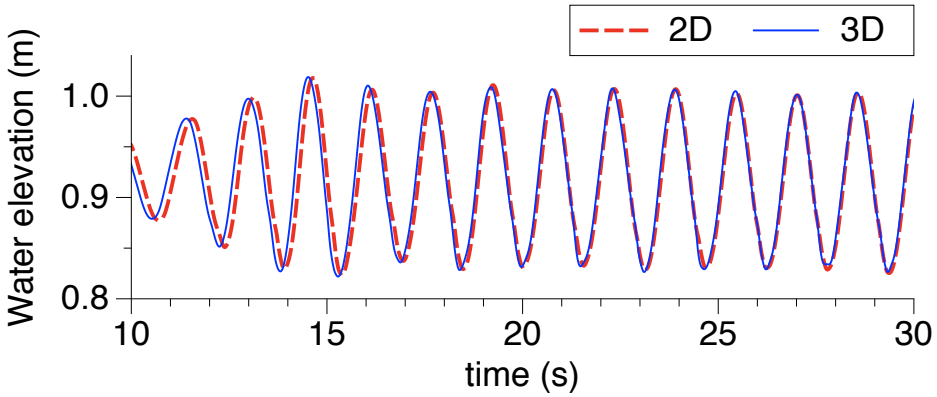

Figure 6: Comparison of free surface motion in 2D and 3D simulations at $\lambda = 3.56$m for the asymmetrical configuration

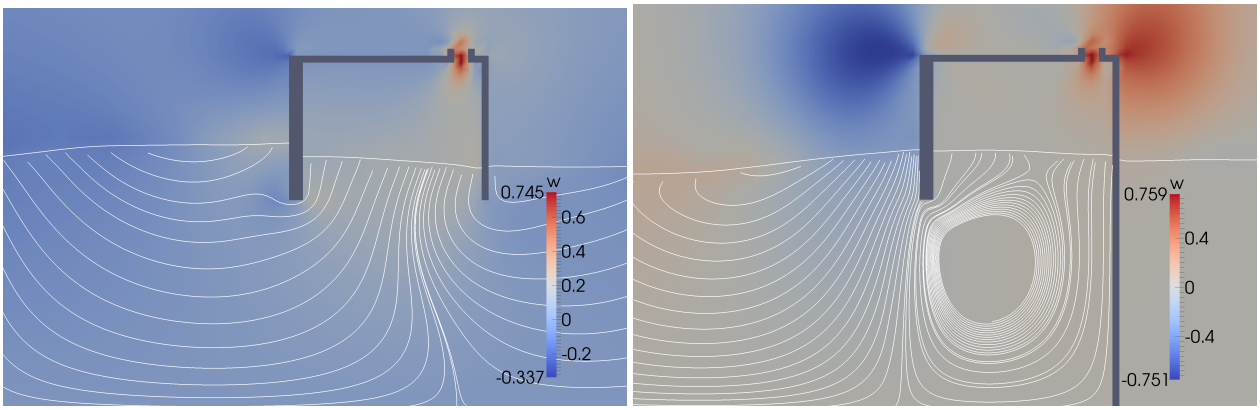

(a) Symmetrical setup **(b)** Asymmetrical setup

Figure 7: Streamlines for $\lambda = 3.56$m at $t = 27$s in the numerical simulation

CONCLUSIONS

The CFD model employed in this study, REEF3D, is able to simulate the working of an OWC device. The wave generation method is found to be satisfactory with accurate wave generation. This is important for OWC simulations because the incident amplitude at the location of the device defines the wave energy available at the device. In order to effectively evaluate the working of the device in terms of hydrodynamic efficiency, the available wave energy has to be calculated correctly.

The effect of asymmetrical and symmetrical configurations of an OWC device is studied. The amplitude of oscillation in the symmetrical configuration is found to be lower than that in the asymmetrical configuration for the same incident wavelengths and amplitude due to wave transmission across the device in the symmetrical configuration.

Three-dimensional simulations are carried out and the free surface motion in the chamber is compared to the free surface motion in the chamber in a two-dimensional simulations and similar motion of the free surface is observed in both the simulations for symmetrical and asymmetrical configurations of the device. Thus, 2D simulations can be used to analyse the fluid motion in the chamber of the device.

The water particle motion in and around the device is studied and it is observed that large zones of stagnation are formed in the chamber due to the effect of the back wall in the case of an asymmetrical configuration.

Further studies are planned to investigate the effect of damping from a power take-off device, performance with waves of higher steepnesses and the influence of vortex formation in the water in and around the walls of the OWC device.

ACKNOWLEDGEMENTS

The authors are thankful to Michael Morris-Thomas, Principal Naval Architect, Worley Parsons, Perth, Australia for the experimental data and helpful discussions. This study has been carried out under the OWCBC project (No. 217622/E20) and the authors are grateful to the grants provided by the Research Council of Norway. This study was supported in part with computational resources at the Norwegian University of Science and Technology (NTNU) provided by NOTUR, http://www.notur.no.

References

P. A. Berthelsen and O. M. Faltinsen. A local directional ghost cell approach for incompressible viscous flow problems with irregular boundaries. *Journal of Computational Physics*, 227:4354–4397, 2008.

H. Bihs. Three-dimensional numerical modeling of local scouring in open channel flow. PhD thesis No. 127, Department of Hydraulic and Environmental Engineering, Norwegian University of Science and Technology, Trondheim, Norway, 2011.

A. Chorin. Numerical solution of the Navier-Stokes equations. *Mathematics of Computation*, 22:745–762, 1968.

E. Didier, J. M. Paix*ão* Conde, and P. R. F. Teixeira. Numerical simulation of an oscillating water column wave energy convertor with and without damping. In *Proc., International Conference on Computational Methods in Marine Engineering*, 2011.

P. A. Durbin. Limiters and wall treatments in applied turbulence modeling. *Fluid Dynamics Research*, 41: 1–18, 2009.

A. P. Engsig-Karup. *Unstructured nodal DG-FEM solution of high-order boussinesq-type equations*. PhD thesis, Technical University of Denmark, Lyngby, 2006.

D. V. Evans. Oscillating water column wave energy convertors. *IMA Journal of Applied Mathematics*, 22: 423–433, 1978.

D. V. Evans. Wave power absorption by systems of oscillating surface pressure distributions. *Journal of Fluid Mechanics*, 114:481–499, 1982.

A. Harten. High resolution schemes for hyperbolic conservation laws. *Journal of Computational Physics*, 49:357–393, 1983.

T. Höhne and C. Vallée. Numerical prediction of horizontal stratified flows. In *Proc., 6th International Conference on CFD in Oil and Gas, Metallurgical and Process industries, Trondheim*, 2008.

K. Hong, S. H. Shin, D. C. Hong, H. S. Choi, and S. W. Hong. Effects of shape parameters of owc chamber in wave energy absorption. In *Proc., 17th International Offshore and Polar Engineering Conference, Lisbon*, 2007.

G. S. Jiang and C. W. Shu. Efficient implementation of weighted ENO schemes. *Journal of Computational Physics*, 126:202–228, 1996.

W. Koo and M. H. Kim. Nonlinear NWT simulation for oscillating water column wave energy convertor. In *Proc., 29th International Conference on Ocean, Offshore and Arctic Engineering, Shanghai*, 2010.

J. Larsen and H. Dancy. Open boundaries in short wave simulations - a new approach. *Coastal Engineering*, 7:285–297, 1983.

Z. Liu, B. Hyun, and K. Hong. Application of numerical wave tank to owc air chamber for wave energy conversion. In *Proc., 18th International Offshore and Polar Engineering Conference, Vancouver*, 2008.

S. Mayer, A. Garapon, and L. S. Sørensen. A fractional step method for unsteady free surface flow with applications to non-linear wave dynamics. *International Journal for Numerical Methods in Fluids*, 28: 293–315, 1998.

F. R. Menter. Two-equation eddy-viscosity turbulence models for engineering applications. *The American Institute of Aeronautics and Astronautics Journal*, 32:1598–1605, 1992.

M. T. Morris-Thomas, R. J. Irvin, and K. P. Thiagarajan. An investigation into the hydrodynamic efficiency of an oscillating water column. *Journal of Offshore Mechanics and Arctic Engineering*, 129:273–278, 2007.

C. S. Peskin. Flow patterns around the heart valves. *Journal of Computational Physics*, 10:252–271, 1972.

A. J. N. A. Sarmento. Wave flume experiments on two-dimensional oscillating water column wave energy devices. *Experiments in Fluids*, 12:286–292, 1992.

A. J. N. A. Sarmento and A. F. O. Falcão. Wave generation by an oscillating surface pressure and its application in wave energy extraction. *Journal of Fluid Mechanics*, 150:467–485, 1985.

U. Senturk and A. Ozdamar. Modelling the interaction between water waves and the oscillating water column wave energy device. *Mathematical and Computational Applications*, 16(3):630–640, 2011.

M. Sussman, P. Smereka, and S. Osher. A level set approach for computing solutions to incompressible two-phase flow. *Journal of Computational Physics*, 114:146–159, 1994.

K. Thiruvenkatasamy and S. Neelamani. On the efficiency of wave energy caissons in array. *Applied Ocean Research*, 19:61–72, 1997.

Y. H. Tseng and J. H. Ferziger. A ghost-cell immersed boundary method for flow in complex geometry. *Journal of Computational Physics*, 192:593–623, 2003.

H. van der Vorst. BiCGStab: A fast and smoothly converging variant of Bi-CG for the solution of nonsymmetric linear systems. *SIAM Journal on Scientific and Statistical Computing*, 13:631–644, 1992.

D. C. Wilcox. *Turbulence modeling for CFD*. DCW Industries Inc., La Canada, California., 1994.

Y. Zhang, Q. P. Zou, and D. Greaves. Air-water two phase flow modelling of hydrodynamic performance of an oscillating water column device. *Renewable Energy*, 41:159–170, 2012.